Linear and nonlinear shape alignment without correspondences

Zoltan Kato

Department of Image Processing and Computer Graphics
University of Szeged
www.inf.u-szeged.hu/~kato/

Problem Statement

- Registration of image pairs is needed whenever one has to compare or align different images of an object
- Applications:
  - object recognition
  - image mosaicing
  - super resolution
  - medical image analysis, …

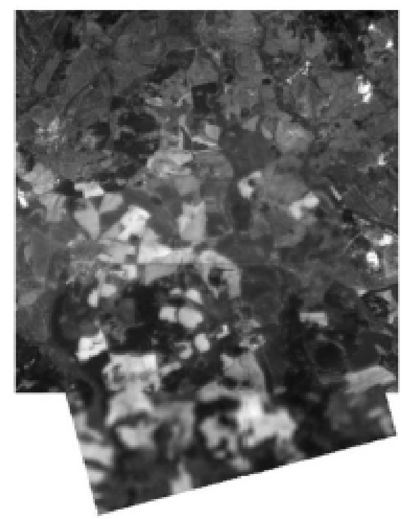

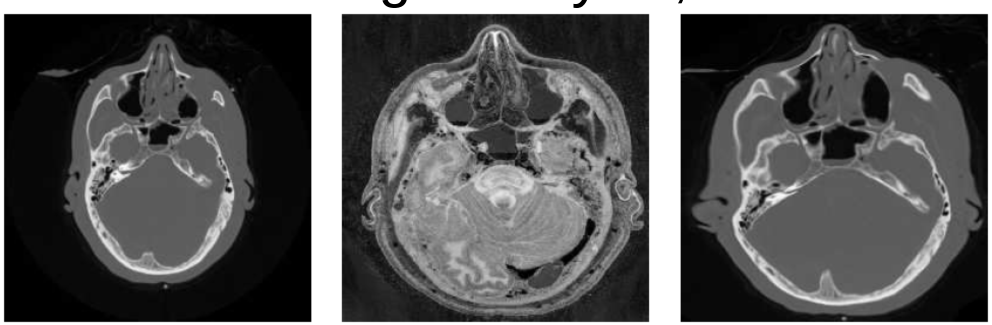

Belongie, S.; Malik, J. & Puzicha, J. **Shape Matching and Object Recognition Using Shape Context**. *IEEE Transactions on Pattern Analysis and Machine Intelligence,* **2002***, 24*, 509-522
Zitová, B. & Flusser, J. **Image Registration Methods: A Survey**. *Image and Vision Computing,* **2003***, 21*, 977-1000
Vandewalle, P.; Sbaiz, L.; Süsstrunka, S. & Vetterli, M. **Registration of aliased images for super-resolution imaging**. *Proc. SPIE/IS&T Visual Comm. & Image Proc. Conf.,* **2006***, 6077*, 13-23
Periaswamy, S. and Farid, H. **Medical Image Registration with Partial Data**. *Medical Image Analysis,* **2006***, 10*, 452-464

Goal: find the aligning transformation

Template

φ

φ^{-1}

Observation (deformed)

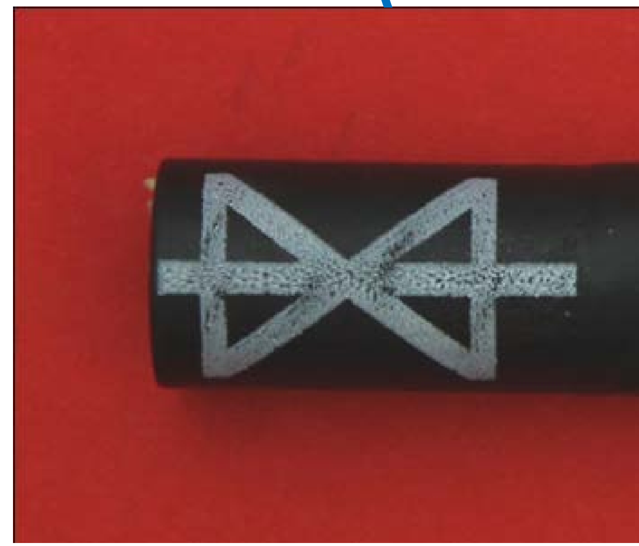

We know (*identity relation*):

$$\mathbf{y} = \varphi(\mathbf{x}) \quad \Leftrightarrow \quad \mathbf{x} = \varphi^{-1}(\mathbf{y})$$

where $\varphi : \mathbb{R}^2 \rightarrow \mathbb{R}^2, \varphi(\mathbf{x}) = [\varphi_1(\mathbf{x}), \varphi_2(\mathbf{x})]^T$

Covariant functions



- If we can observe some image features, g(x) and h(y), (*e.g.* gray-level of the pixels [Hagege-Francos2010]) that are ***covariant*** under the transformation, then

$$g(x) = h(\varphi(x)) = h(y)$$

  - Lack of characteristic features (*e.g.* binary images, printed art)
  - Changes in features (*e.g.* illumination changes, multimodality)

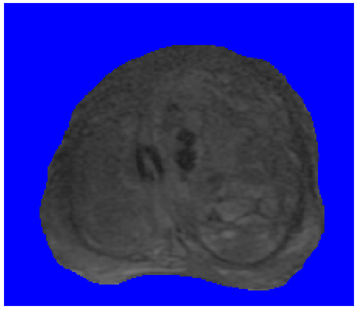
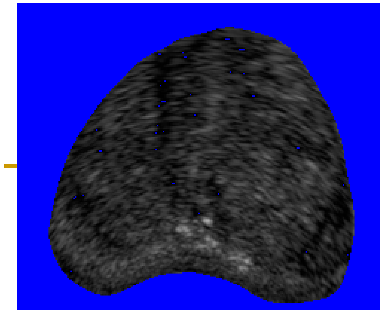

R. Hagege, J. M. Francos, **Parametric estimation of affine transformations: An exact linear solution**, *Journal of Mathematical Imaging and Vision* 37 (1) (2010) 1–16.

Classical approach

$$\arg\min_{\varphi} \left\| Templ. - \varphi(Obs.) \right\|, \text{ where } \varphi : R^2 \rightarrow R^2$$

- Common components:

a. *Feature space*
   - Landmarks (*e.g.* corners, line crossing, etc.)
   - *Object descriptors* (*e.g.* moments)

b. *Space of transformations*
   - Rigid-body, *affine*, projective, elastic, …

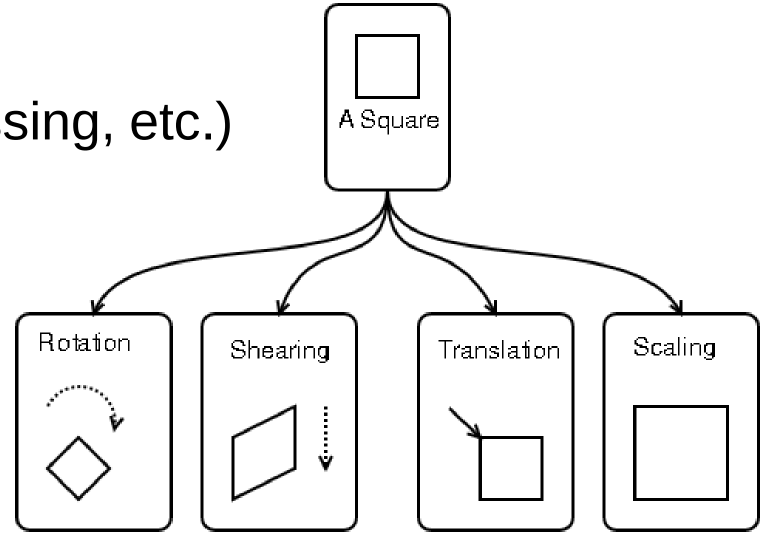

c. *Search strategy*
   - Initialization + optimization (local minima)

d. *Similarity metric* over the feature space

http://www.gnome.org/~mathieu/libart/libart-affine-transformation-matrices.html

Classical approach issues

- Optimization yields local minima
- Common assumptions:
  - deformation is close to identity
  - Landmark extraction based on local descriptors ➔ need for rich and characteristic radiometric information (SIFT, SURF,…)
- What if these assumptions are invalid or landmark extraction/matching is unreliable?

Solution without correspondences

Find a solution without establishing correspondences!

$$\mathbf{y} = \varphi(\mathbf{x})$$

integrate out individual point correspondences over the foreground regions $\mathcal{F}_t$ and $\mathcal{F}_o$.

$$\int_{\mathcal{F}_o} \mathbf{y}\, d\mathbf{y} = \int_{\mathcal{F}_t} \varphi(\mathbf{x})\, |J_\varphi(\mathbf{x})|\, d\mathbf{x}$$

where the integral transformation $\mathbf{y} = \varphi(\mathbf{x}), d\mathbf{y} = |J_\varphi(\mathbf{x})|\, d\mathbf{x}$ has been applied, $|J_\varphi| : \mathbb{R}^2 \to \mathbb{R}$ is Jacobian determinant

This nonlinear system of two equations (for $y_i, \varphi_i(\mathbf{x}),\ i = 1, 2$) is not enough to solve for more than 2 unknowns!

Generating equations

- Space of allowed deformations is low dimensional (~number of free parameters)!

Basic idea: generate more linearly independent equations by making use of a set of nonlinear ω functions:

$$\mathbf{y} = \varphi(\mathbf{x}) \rightarrow \omega(\mathbf{y}) = \omega(\varphi(\mathbf{x}))$$

Let $\omega_i : \mathbb{R}^2 \rightarrow \mathbb{R} (i = 1, \ldots, \ell)$ a set of nonlinear functions. We obtain the following system of equations:

$$\int_{\mathcal{F}_o} \omega_i(\mathbf{y}) d\mathbf{y} = \int_{\mathcal{F}_t} \omega_i(\varphi(\mathbf{x})) \left| J_\varphi(\mathbf{x}) \right| d\mathbf{x}$$

Interpretation

- Intuitively, each ω generates a consistent coloring of the shapes
- The equations match the volume of the applied ω function over the shapes.
- The parameters of the aligning transformation are then simply obtained as the solution of the nonlinear system of equations.

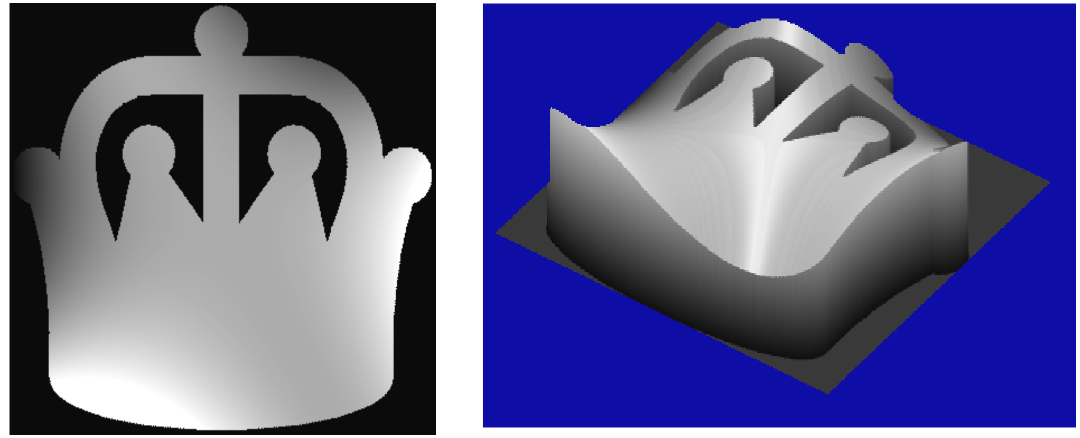

polynomial

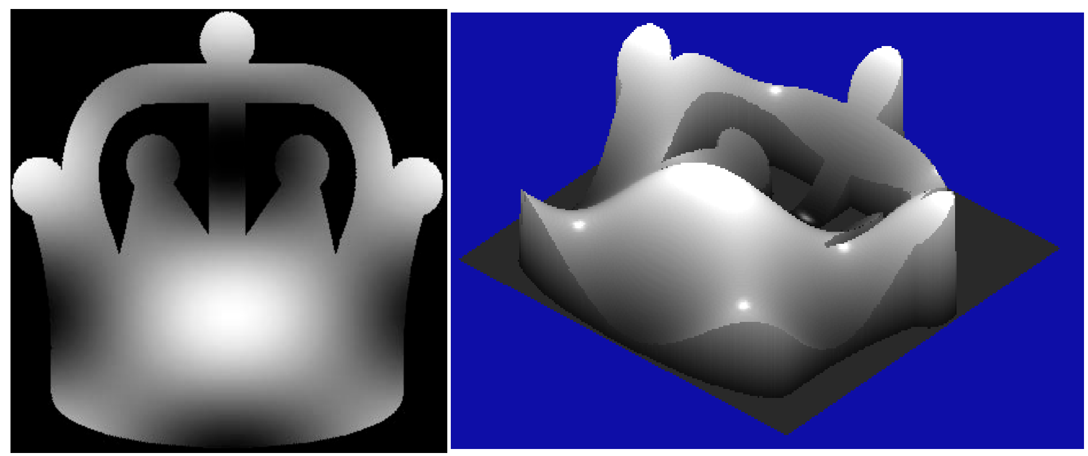

trigonometric

How to choose the ω set?

- From a theoretical point of view, only trivial restrictions:
  - Integrable, rich enough
  - Unbiased: each equation has a balanced contribution to the algebraic error:
    - Images normalized
    - Range of ω functions normalized
- From a practical point of view: In general, we have to solve a system of integral equations
  - ➔ need to evaluate intermediate deformations
  - ➔ complexity is highly dependent on image size

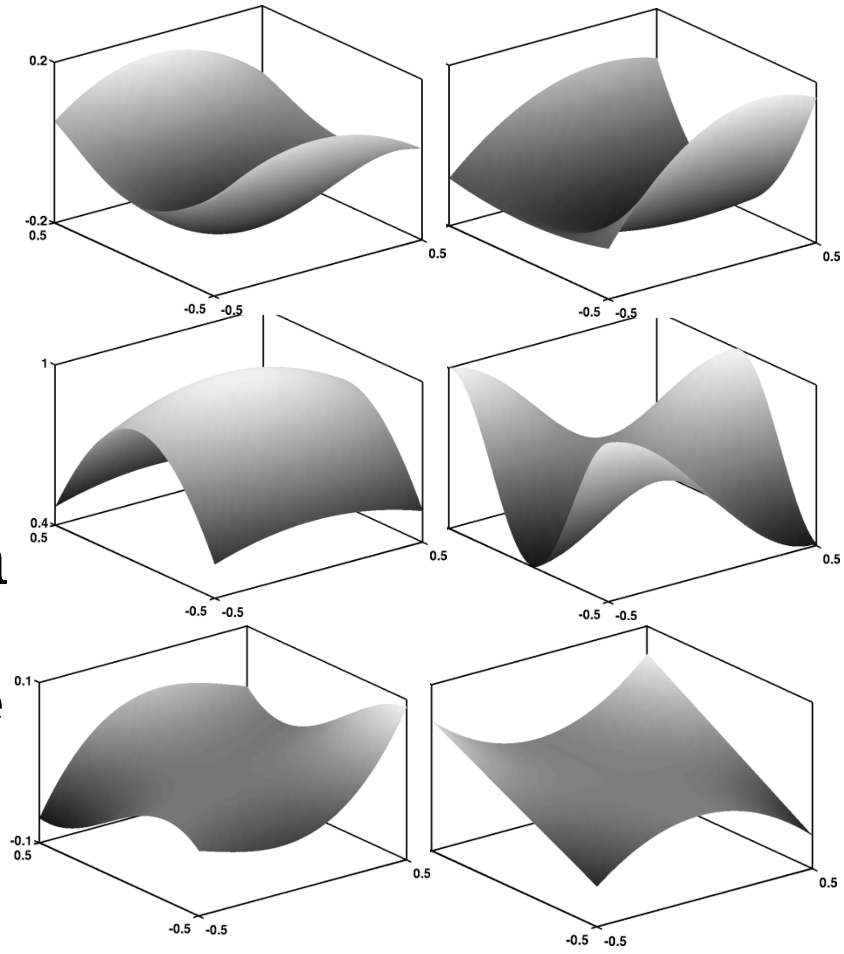

How to choose the ω set?

- Can it be reduced to a plain polynomial system?
  - Need to scan the images only once ➔ considerable speed-up (complexity almost independent of the image size!)
- Yes, if
  - Deformation is given as a linear combination of basis functions
    - polynomial or thin plate spline deformations
    - other diffeomorphisms can be approximated by their Taylor expansion
  - Adopted ω functions are polynomial [PAMI2011].

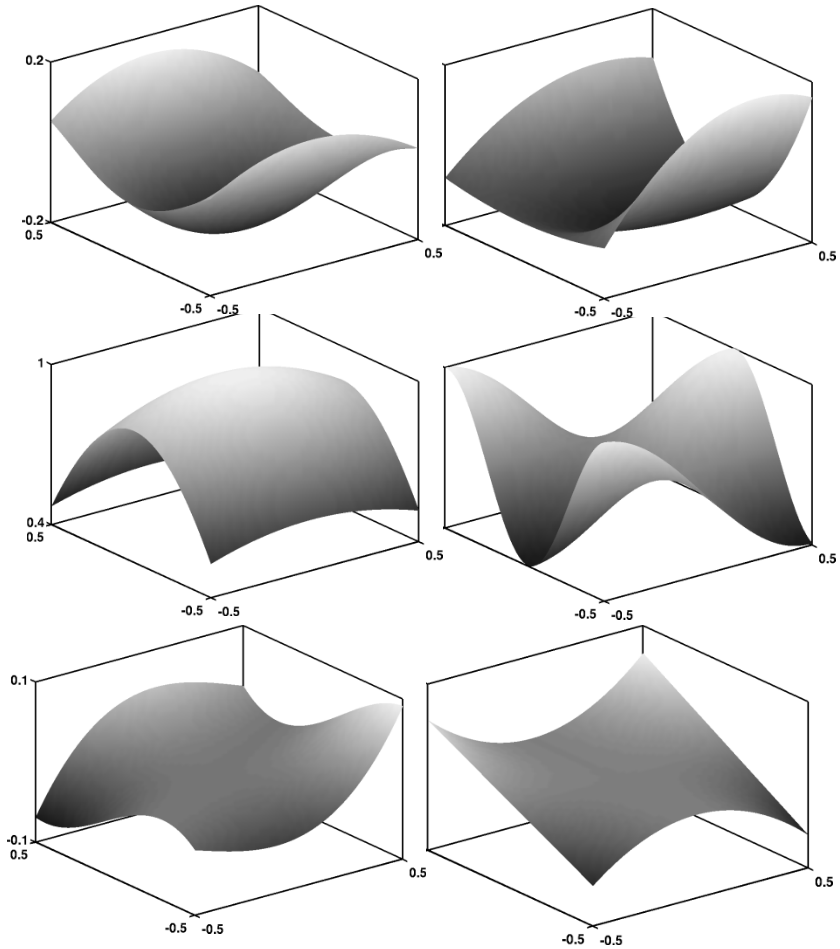

Templates

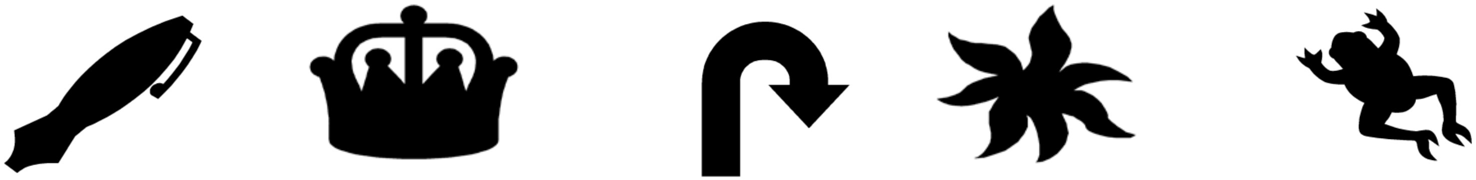

Observations

Shape Context[2]

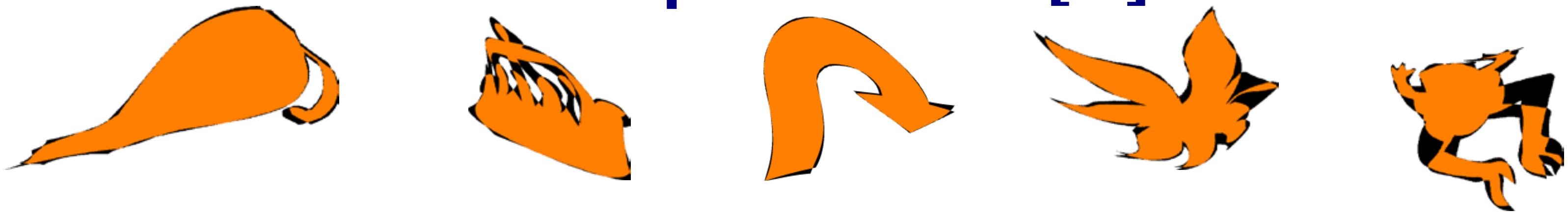

Proposed method

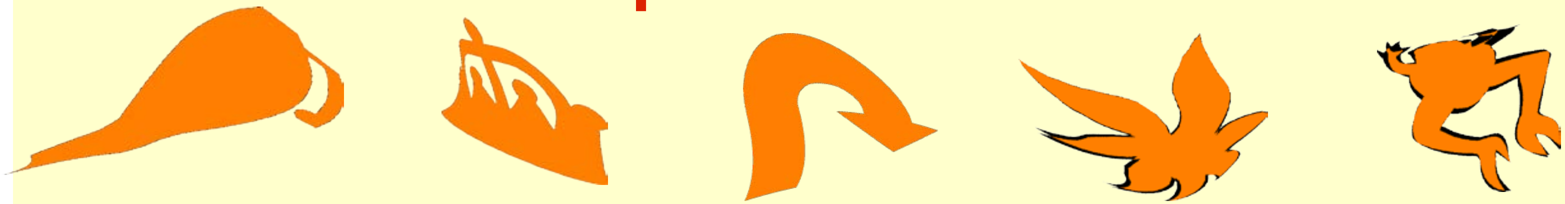

Linear (affine) deformations

- We use homogeneous coordinates. Identity relation:

$$\mathbf{y} = \mathbf{A}\mathbf{x} \quad \Leftrightarrow \quad \mathbf{x} = \mathbf{A}^{-1}\mathbf{y}$$

- Transformation matrix:

$$\mathbf{A} = \begin{pmatrix} a_{11} & a_{12} & a_{13} \\ a_{21} & a_{22} & a_{23} \\ 0 & 0 & 1 \end{pmatrix} \text{ and } \mathbf{A}^{-1} = \begin{pmatrix} q_{11} & q_{12} & q_{13} \\ q_{21} & q_{22} & q_{23} \\ 0 & 0 & 1 \end{pmatrix}$$

$$\int_{\mathcal{D}} \mathbf{x} d\mathbf{x} = \frac{1}{|\mathbf{A}|} \int_{\mathcal{F}} \mathbf{A}^{-1}\mathbf{y} d\mathbf{y}$$

- Expanding (k=1,2):

$$|\mathbf{A}| \int_{\mathcal{D}} x_k d\mathbf{x} = q_{k1} \int_{\mathcal{F}} y_1 d\mathbf{y} + q_{k2} \int_{\mathcal{F}} y_2 d\mathbf{y} + q_{k3} \int_{\mathcal{F}} d\mathbf{y}$$

Computing the Jacobian

- Jacobian: (absolute value of the transformation's determinant)

$$\mathbb{1}_t(\mathbf{x}) = \mathbb{1}_o(\mathbf{A}\mathbf{x}) = \mathbb{1}_o(\mathbf{y})$$

$$\mathbf{x} = \mathbf{A}^{-1}\mathbf{y},\ d\mathbf{x} = d\mathbf{y}/|\mathbf{A}|$$

$$\int_{\mathbb{P}^2} \mathbb{1}_t(\mathbf{x})d\mathbf{x} = \frac{1}{|\mathbf{A}|}\int_{\mathbb{P}^2} \mathbb{1}_o(\mathbf{y})d\mathbf{y} \quad \Rightarrow \quad |\mathbf{A}| = \frac{\int_{\mathcal{F}} d\mathbf{y}}{\int_{\mathcal{D}} d\mathbf{x}}$$

- Sign ambiguity
  (we assume that |J|>0)

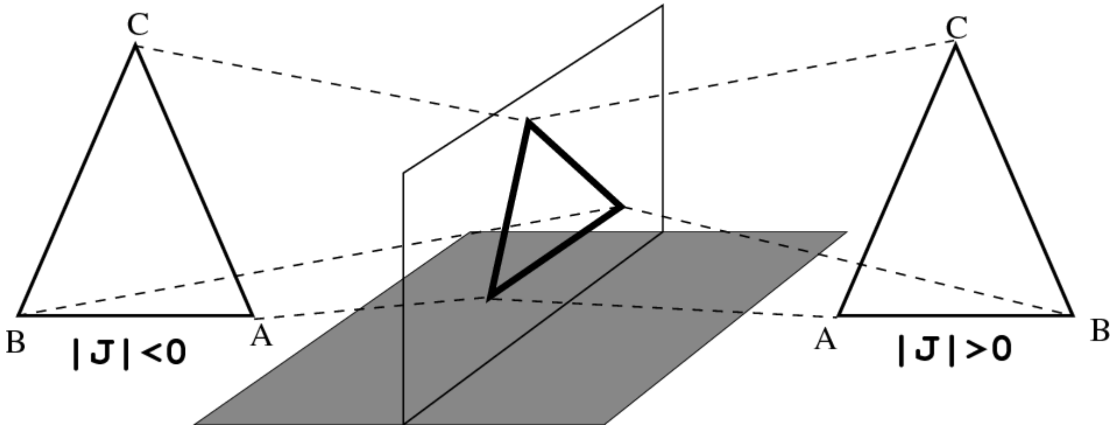

Proposed polynomial solution

- 2 equations but 6 unknows: $$\int_{\mathcal{D}} \mathbf{x} d\mathbf{x} = \frac{1}{|\mathbf{A}|} \int_{\mathcal{F}} \mathbf{A}^{-1} \mathbf{y} d\mathbf{y}$$
- How to generate 4 more linearly independent eq?
  - ➔Using ***Invariant function*** $\omega : \mathbb{P}^2 \rightarrow \mathbb{P}^2$

$$\omega(\mathbf{x}) = \omega(\mathbf{A}^{-1}\mathbf{y})$$

$$\int_{\mathcal{D}} \omega(\mathbf{x}) d\mathbf{x} = \frac{1}{|\mathbf{A}|} \int_{\mathcal{F}} \omega(\mathbf{A}^{-1}\mathbf{y}) d\mathbf{y}$$

$\omega(\mathbf{x}) = \mathbf{x}$ $\omega(\mathbf{x}) = [x_1^2, x_2^2, 1]^T$ $\omega(\mathbf{x}) = [x_1^3, x_2^3, 1]^T$

Polynomial system of equations

- Polynoms are prefect choise for ω
- Separated system of (polynomial) equations:
  - Using the basic properties of the Lebesgue integral
  - n = 1,2,3; k = 1,2

$$|\mathbf{A}| \int x^n = \sum_{i=1}^{n} \binom{n}{i} \sum_{j=0}^{i} \binom{i}{j} q_{k1}^{n-i} q_{k2}^{i-j} q_{k3}^{j} \int y_1^{n-i} y_2^{i-j}$$

  - Linear deformation with polynomial ω yields standard 1st, 2nd, and 3rd order shape moments:

$$|\mathbf{A}| \int x_k = q_{k1} \int y_1 + q_{k2} \int y_2 + q_{k3} \int 1,$$

$$|\mathbf{A}| \int x_k^2 = {q_{k1}}^2 \int y_1^2 + {q_{k2}}^2 \int y_2^2 + {q_{k3}}^2 \int 1 + 2 q_{k1} q_{k2} \int y_1 y_2 + 2 q_{k1} q_{k3} \int y_1 + 2 q_{k2} q_{k3} \int y_2,$$

$$|\mathbf{A}| \int x_k^3 = {q_{k1}}^3 \int y_1^3 + {q_{k2}}^3 \int y_2^3 + {q_{k3}}^3 \int 1 + 3 {q_{k1}}^2 q_{k2} \int y_1^2 y_2 + 3 {q_{k1}}^2 q_{k3} \int y_1^2 + 3 {q_{k2}}^2 q_{k3} \int y_2^2$$
$$+ 3 q_{k1} {q_{k2}}^2 \int y_1 y_2^2 + 3 q_{k2} {q_{k3}}^2 \int y_2 + 3 q_{k1} {q_{k3}}^2 \int y_1 + 6 q_{k1} q_{k2} q_{k3} \int y_1 y_2.$$

Numerical implementation

- Approximate the integral: $\mathcal{D} \approx D = \{\mathbf{d}^i\}_{i=1}^n$

$$\int_{\mathcal{D}} x_k d\mathbf{x} \approx \sum_{i=1}^{n} \mathbf{d}_k^i$$

- Jacobian: $|\mathbf{A}| = \frac{m}{n}$
- **Algorithm**:
  1. Estimating the Jacobian
  2. Evaluating the integrals provides the coefficient of the unknowns
  3. Solving the system of equations

- Time complexity: $\mathcal{O}(N)$, where N is the number of the foreground pixel

Experimental results

- Dataset: (43344 images with size of 1000 x 1000)
  - 56 different shapes

Rotations:	$0°, 60°, \ldots, 240°$	Shearings:	$0, 0.5, 1$
Scalings:	$0, 0.5, \ldots, 2$	Translations:	$0, 20$

  - Filled: 28638, line drawings: 14706
- Measures of error:
  - **A**: transformation, $\widehat{\mathbf{A}}$: estimated transformation, *D*: domain

$$\epsilon = \frac{1}{|D|} \sum_{\mathbf{p} \in D} \frac{\|(\mathbf{A} - \widehat{\mathbf{A}})\mathbf{p}\|}{\|\mathbf{A}\mathbf{p}\|}$$

  - R: *registered*, O: *observation*, Δ: symmetric difference

$$\delta = \frac{|R \triangle O|}{|R| + |O|} \cdot 100\%$$

Experimental results

- Results on the whole dataset

	Runtime (sec.)	ϵ (pixel)	δ (%)
Median	1.41	2.81	0.76
Mean	1.75	116.14	6.36
Variance	2.28	2643.22	17.02

- Comparison to related approaches
  - 1000 randomly chosen image
  - Matlab implementation

	Runtime (sec.)	ϵ (pixel)	δ (%)
Kannala *et al.* [10]	107.19	50.92	21.46
Shape context [7]	57.45	–	15.17
Proposed	1.06	2.87	0.42

Kannala, J.; Rahtu, E.; Heikkilä, J. & Salo, M. **A New Method for Affine Registration of Images and Point Sets.** *LNCS, Proc. of SCIA, Springer,* **2005**, *3540*, 224-234
Belongie, S.; Malik, J. & Puzicha, J. **Shape Matching and Object Recognition Using Shape Context**. *IEEE Transactions on Pattern Analysis and Machine Intelligence,* **2002**, *24*, 509-522

Experimental results: comparison

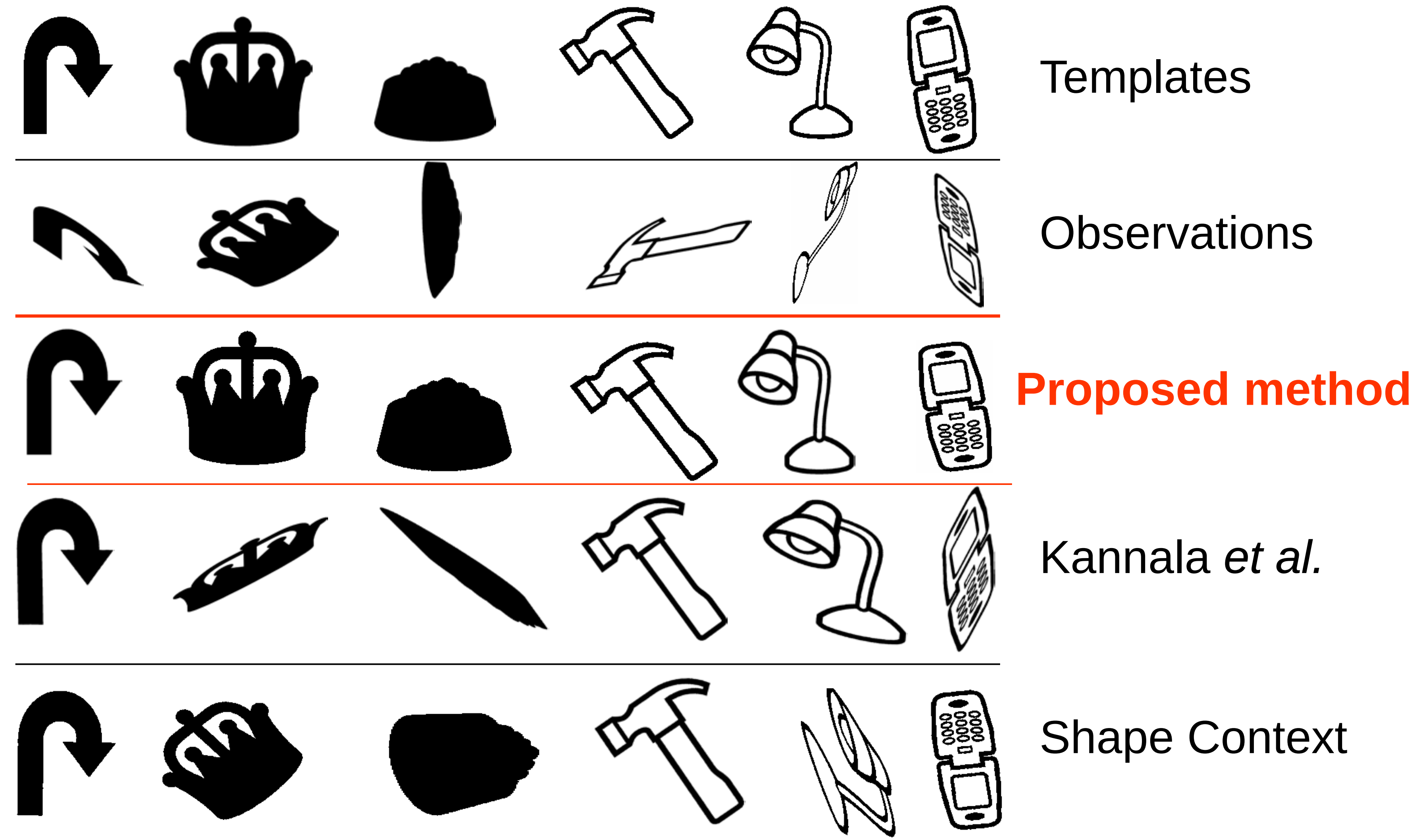

Noise sensitivity

- Geometric noise (i.i.d. additive Gaussian) over the coordinates:

$$\mathbf{y}^* = \mathbf{y} + \varepsilon(\mathbf{y}) = \mathbf{A}\mathbf{x} + \varepsilon^*(\mathbf{y}^*) \Leftrightarrow \mathbf{x} = \mathbf{A}^{-1}\left(\mathbf{y}^* - \varepsilon^*(\mathbf{y}^*)\right)$$

$$\varepsilon(\mathbf{y}) \equiv \varepsilon^*(\mathbf{y}^*) = \left[\varepsilon_1^*(\mathbf{y}^*), \varepsilon_2^*(\mathbf{y}^*), 0\right]^T$$

- ε_1^* and ε_2^* are independent and normally distributed with 0 means and variance σ_1 and σ_2 respectively

$\sigma=5$ $\sigma=10$ $\sigma=20$

Experimental results: noise

- System of equation in the presence of noise:

$$
\begin{aligned}
|\mathbf{A}| \int x_k d\mathbf{x} &= \int (A_k^{-1}\mathbf{y}) d\mathbf{y} \\
|\mathbf{A}| \int x_k^2 d\mathbf{x} &= \int (\mathbf{A}_k^{-1}(\mathbf{y}))^2 d\mathbf{y} + \boxed{q_{k1}^2\sigma_1^2 + q_{k2}^2\sigma_2^2} \\
|\mathbf{A}| \int x_k^3 d\mathbf{x} &= \int (\mathbf{A}_k^{-1}(\mathbf{y}))^3 d\mathbf{y} + \boxed{3q_{k1}^2 q_{k3}\sigma_1^2 + 3q_{k2}^2 q_{k3}\sigma_2^2}
\end{aligned}
$$

- Median of error measures versus σ of the noise on 1000 randomly selected images:

σ	ϵ (pixel)	δ (%)
1	2.73	0.38
2	2.85	0.41
5	3.23	0.73
10	4.43	2.43
20	31.43	13.73
30	195.95	25.84
50	372.64	44.29

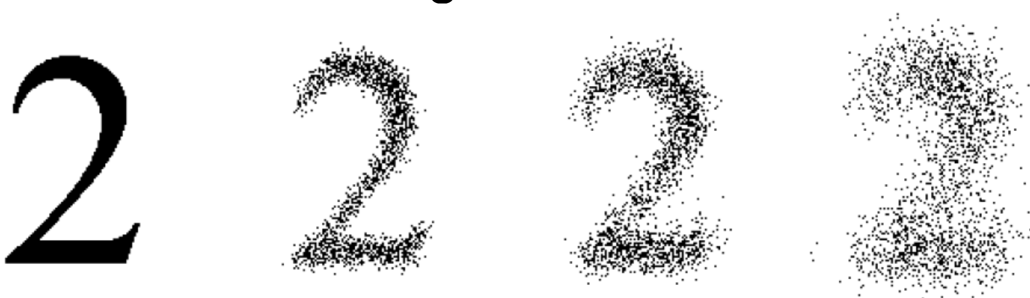

σ=5 σ=10 σ=20

Hip prosthesis registration

- **Challenges**:
  - X-Ray images has a highly nonlinear radiometric distortion
    - Gray-level-based methods are unstable
    - Segmentation is straightforward
      ➔Binary registration
  - Projective mapping
    - Rigid-body transformation in 3D
    - Standard position
      ➔Affine transformation is a good approximation

Hip prosthesis registration (fusion)

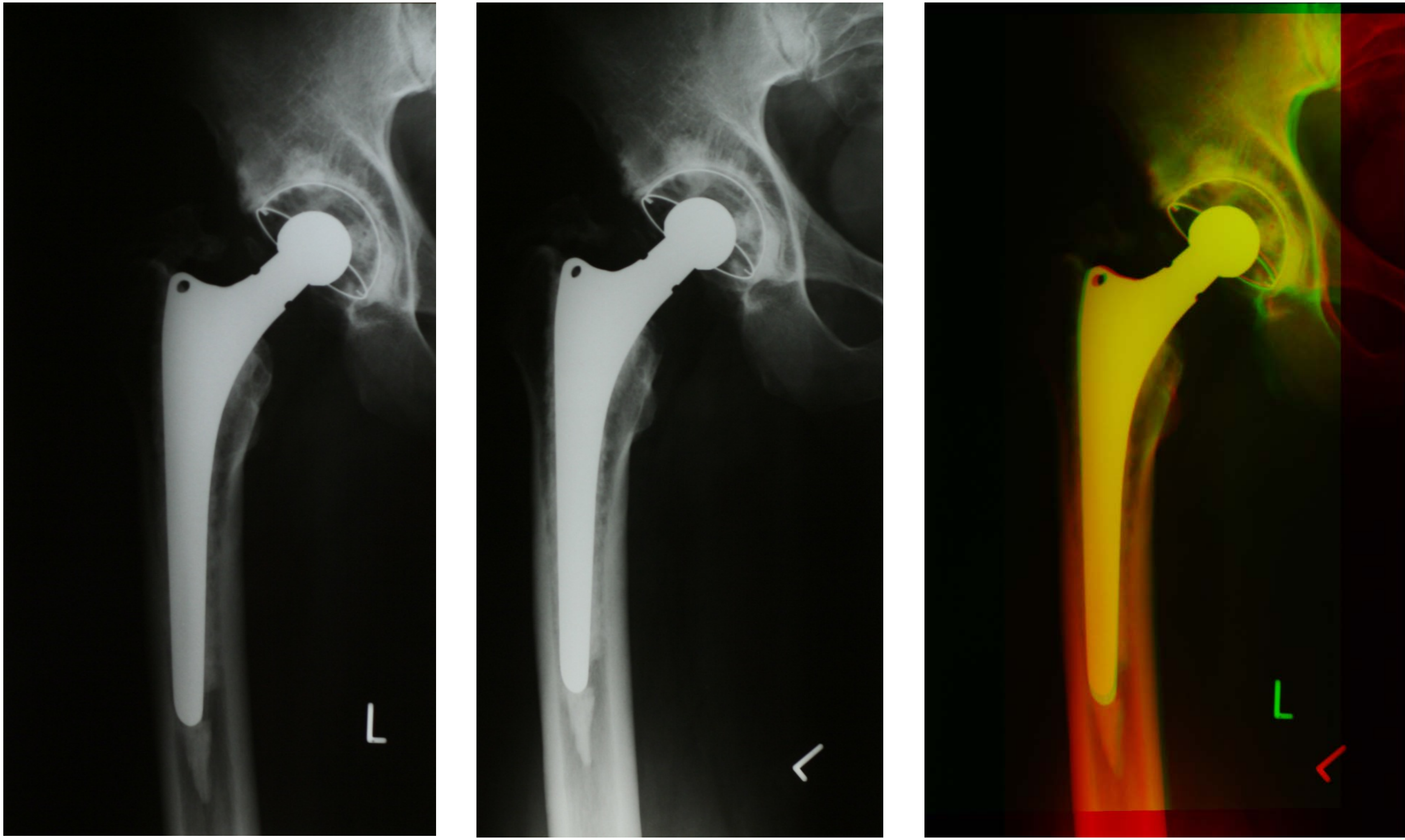

Hip prosthesis registration (fusion)

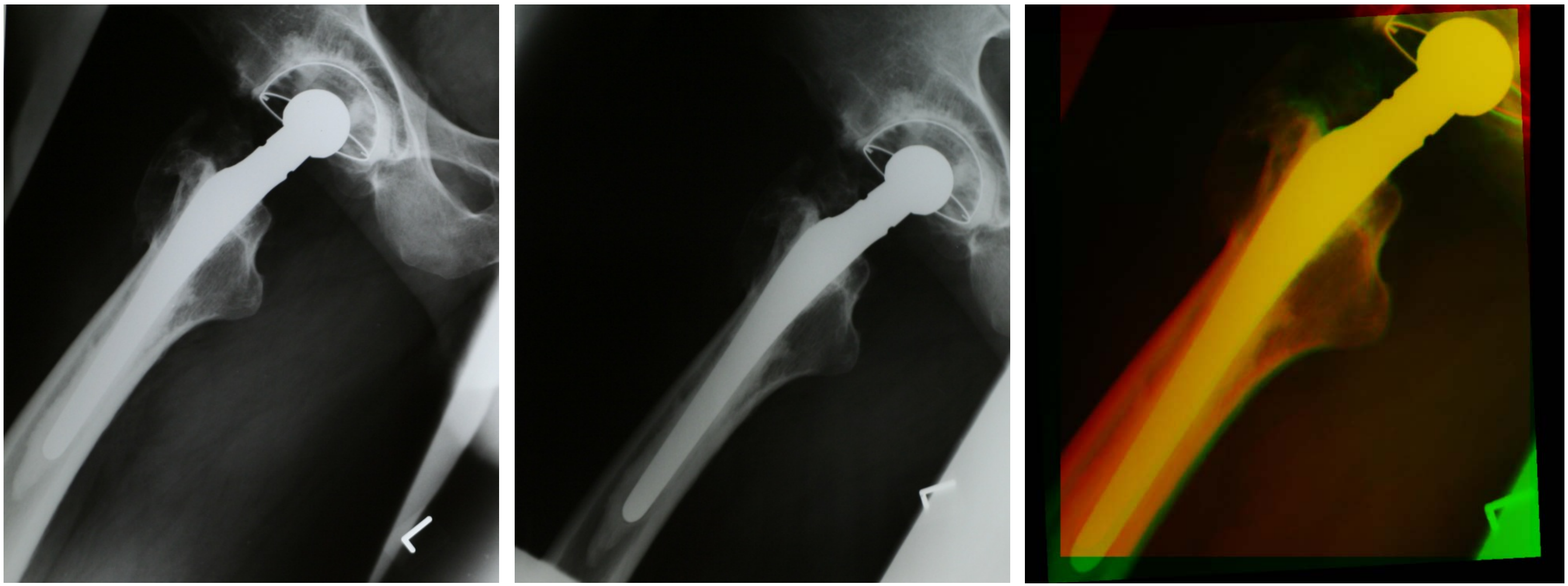

Works also in 3D!

- Each ω generates 1 polynomial equation, a total of 19
  - To ensure more numerical stability, the inverse formulation yields another 19 equations, a total of 38

Independent from transformation parameters: can be precomputed (geometric moments)

$$|\mathbf{A}| \int_{\mathcal{F}_t} x_a \, d\mathbf{x} = \sum_{i=1}^{4} q_{ai} \int_{\mathcal{F}_o} y_i \, d\mathbf{y}$$

$$|\mathbf{A}| \int_{\mathcal{F}_t} x_a x_b \, d\mathbf{x} = \sum_{i=1}^{4} \sum_{j=1}^{4} q_{ai} q_{bj} \int_{\mathcal{F}_o} y_i y_j \, d\mathbf{y}$$

$$|\mathbf{A}| \int_{\mathcal{F}_t} x_a x_b x_c \, d\mathbf{x} = \sum_{i=1}^{4} \sum_{j=1}^{4} \sum_{k=1}^{4} q_{ai} q_{bj} q_{ck} \int_{\mathcal{F}_o} y_i y_j y_k \, d\mathbf{y}$$

$$1 \leq a, b, c \leq 3, \; a \leq b \leq c$$

Samples from the synthetic observations

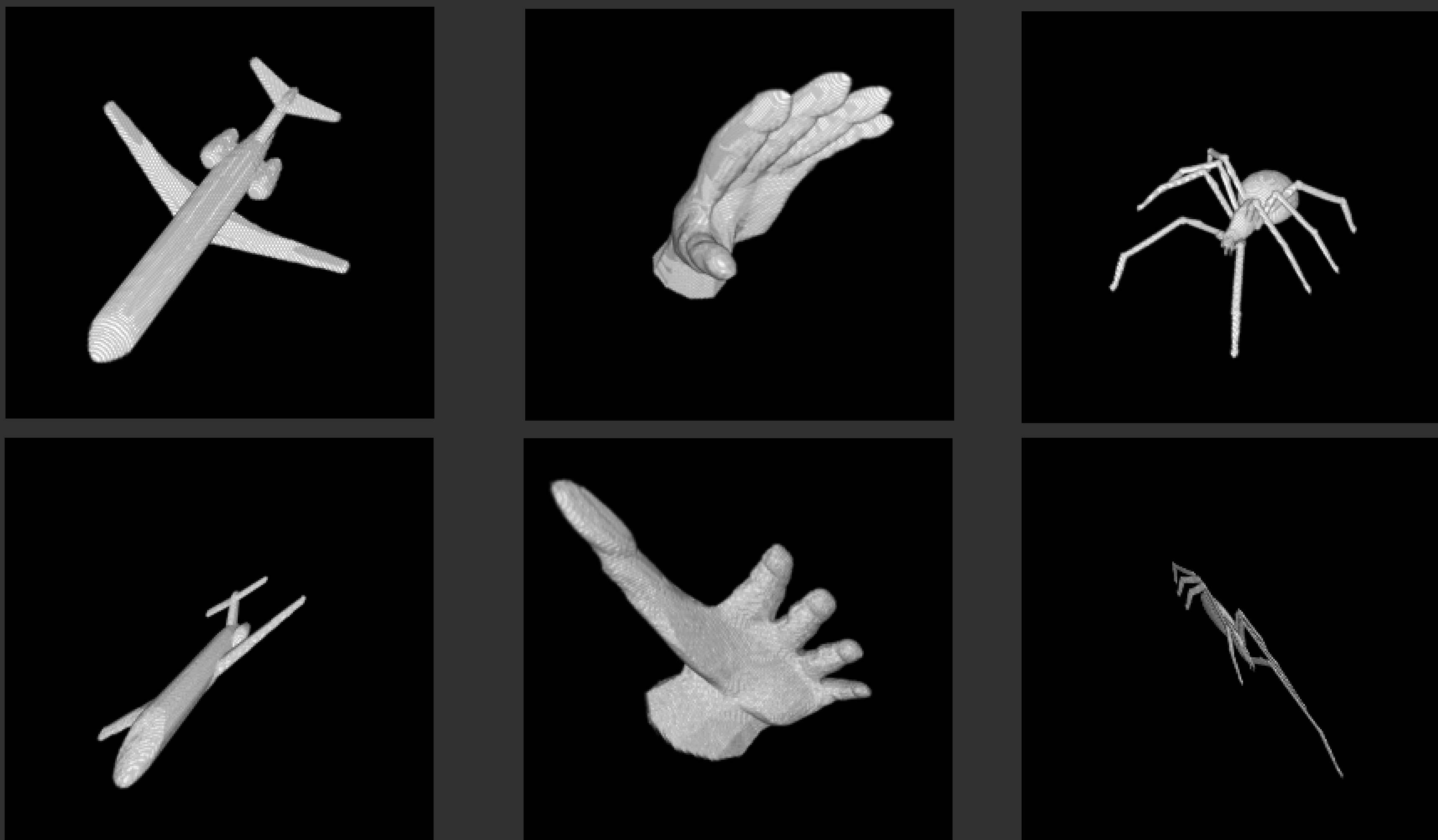

Robustness tests

- Three types of segmentation errors were simulated
  - Missing voxels : even for 90% the results are acceptable

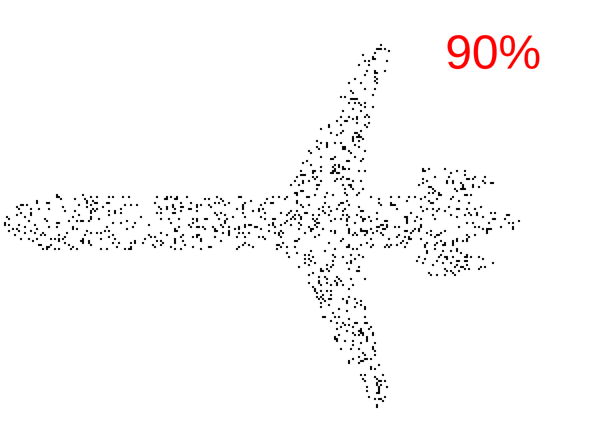

Robustness tests

- Three types of segmentation errors were simulated
  - Missing voxels : even for 90% the results are acceptable
  - Occlusion (Missing volume) : max. 1-2% degradation

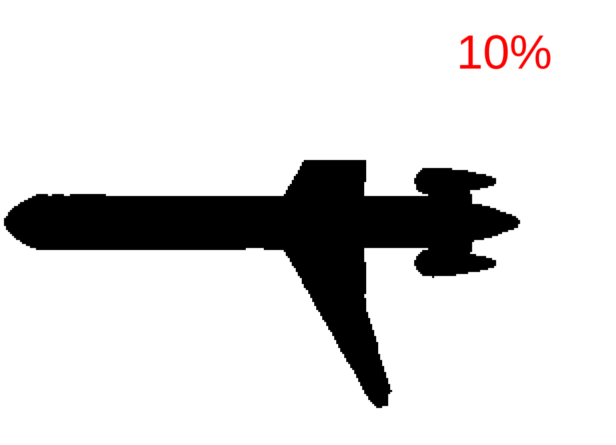

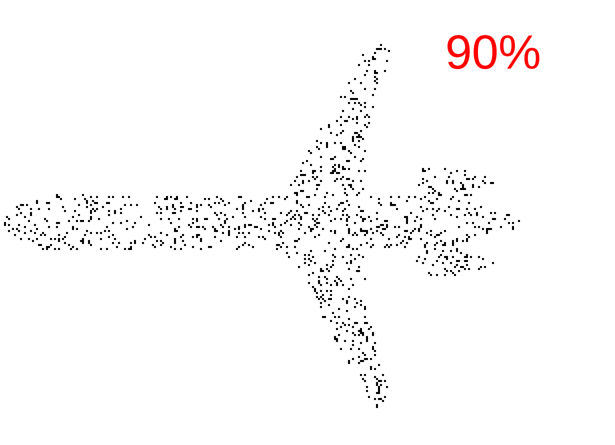

Robustness tests

- Three types of segmentation errors were simulated
  - Missing voxels : even for 90% the results are acceptable
  - Occlusion (Missing volume) : max. 1-2% degradation
  - Surface error: 25% degradation, 70% acceptable registration results (δ<10%)

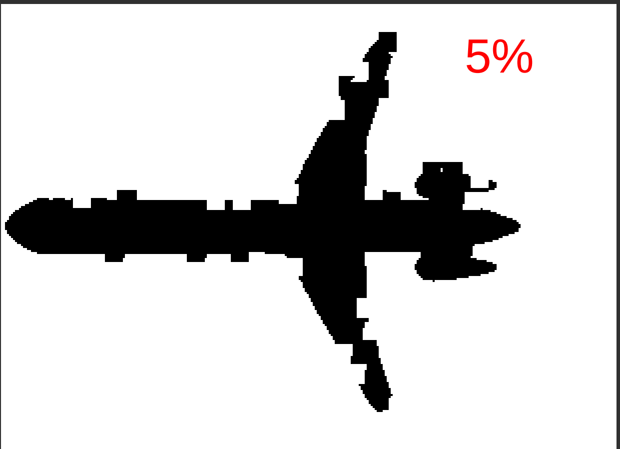

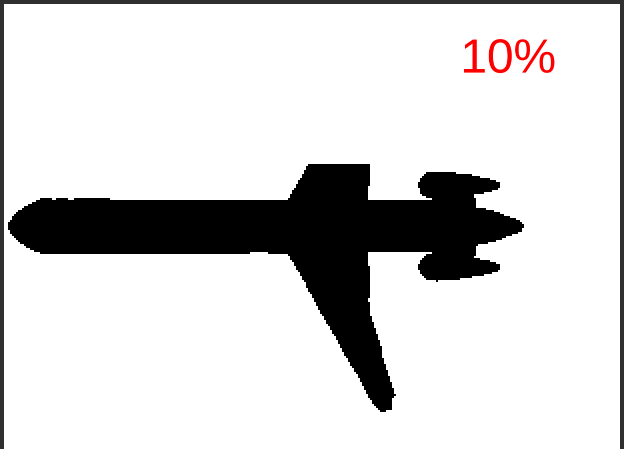

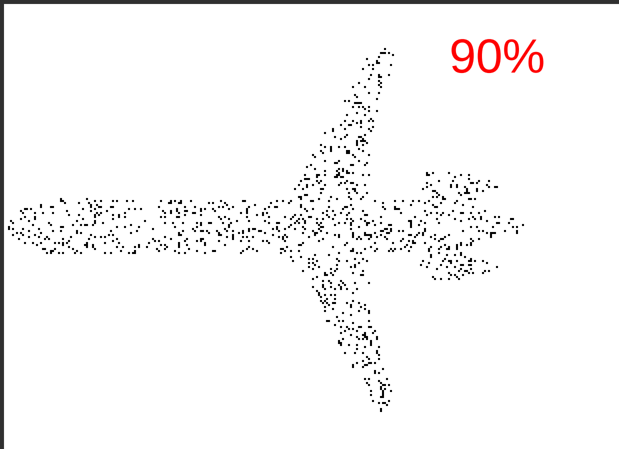

3D CT Registration Result #1

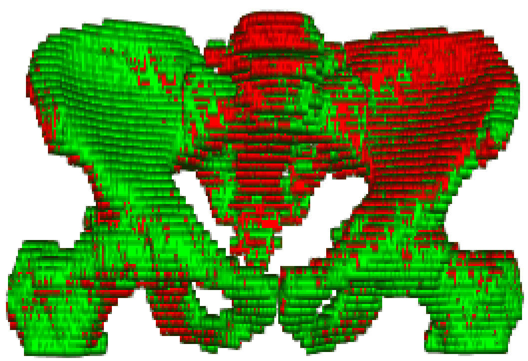

CT study: 512x512x39; 0.68x0.68x5.0; cca. 400.000 object points
Delta error: 14%
Computing time: below 0.1 sec
Computer: Desktop PC with Intel Core2 Duo E6550 CPU @ 2.33 GHz (4 years old)

3D CT Registration Result #4

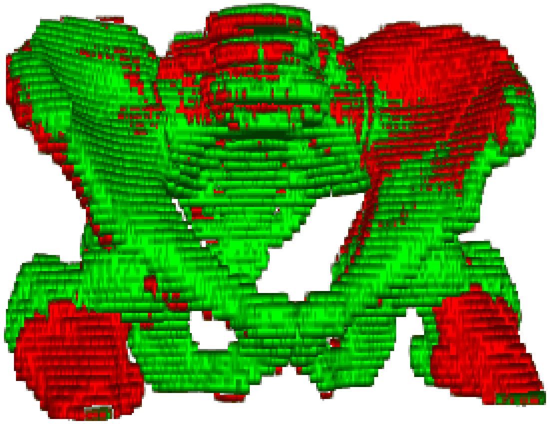

CT study: 512x512x43; 0.79x0.79x5.00 mm; cca. 460.000 object points
Delta error: 32%
Computing time: cca. 0.1 sec

<u>Wrong femur position!</u>

Affine Puzzle: Realigning Deformed Object Fragments without Correspondences

- **<u>Puzzle problem</u>**: reassembling an object from its affine-deformed fragments
  - A *template* and all fragments are available
  - each fragment is subject to a different *n*-dimensional **affine** deformation
- **<u>Challenges</u>**:
  - **partitioning** of the *template* is **unknown**
  - **correspondences** between *template* parts and fragments are **unknown**
  - Segmentation and modeling **errors**
- **<u>Solution</u>**:
  - Problem is reformulated as a **polynomial system of equations**
  - **LSE solution** directly provides the aligning transformations

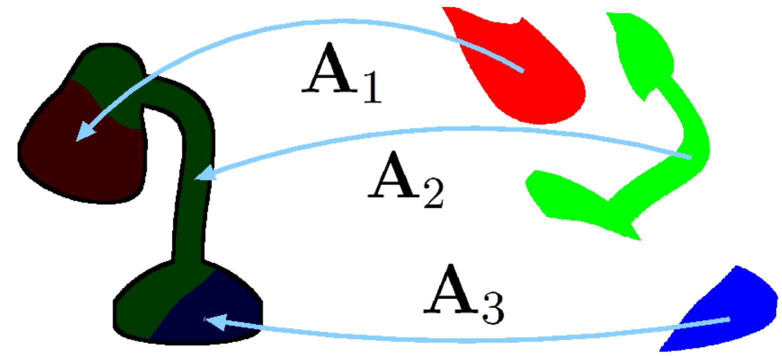

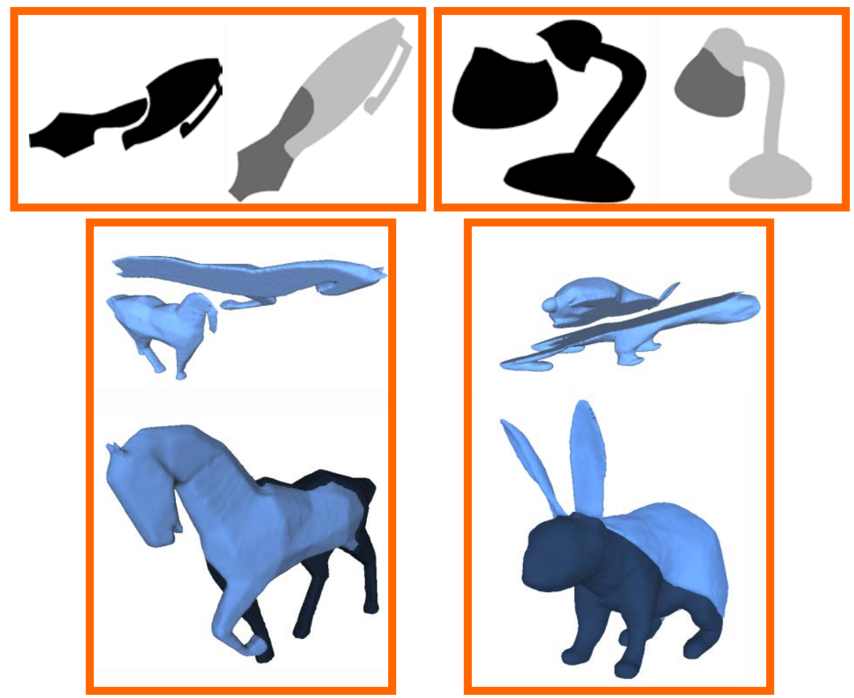

Affine Puzzle: Realigning Deformed Object Fragments without Correspondences

- **<u>Puzzle problem</u>**: reassembling an object from its affine-deformed fragments
  - A *template* and all fragments are available
  - each fragment is subject to a different *n*-dimensional **affine** deformation
- **<u>Challenges</u>**:
  - **partitioning** of the *template* is **unknown**
  - **correspondences** between *template* parts and fragments are **unknown**
  - Segmentation and modeling **errors**
- **<u>Solution</u>**:
  - Problem is reformulated as a **polynomial system of equations**
  - **LSE solution** directly provides the aligning transformations

- Tangram puzzle - 2D affine

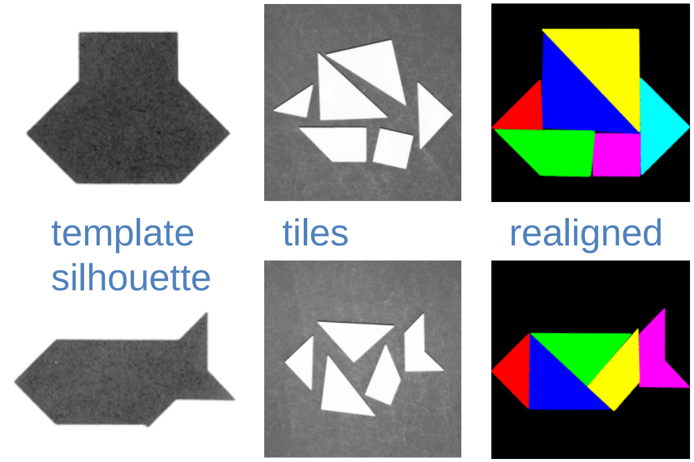

- Bone fracture - 3D rigid body

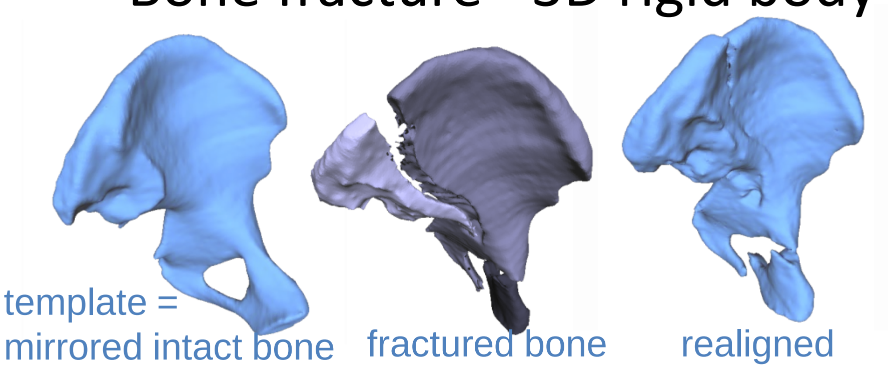

Planar homography

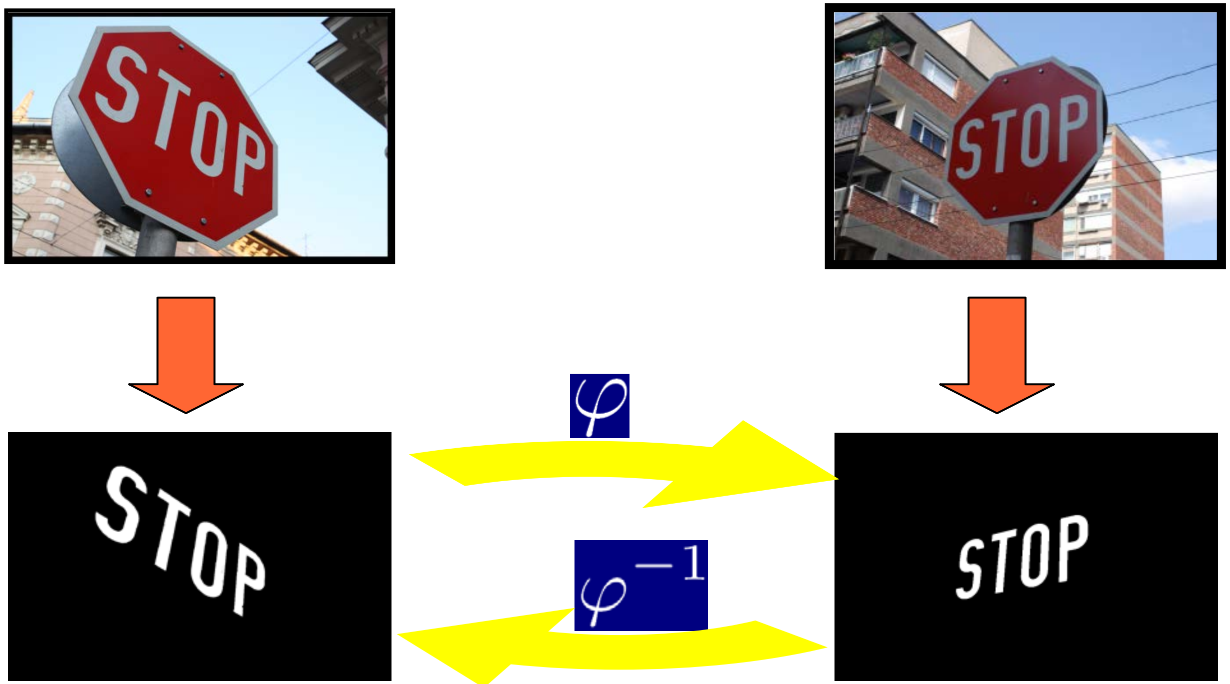

$$\mathbf{y}' = \mathbf{H}\mathbf{x}' \quad \Leftrightarrow \quad \mathbf{x}' = \mathbf{H}^{-1}\mathbf{y}'$$

$$|J_\varphi(\mathbf{x})| = \begin{vmatrix} \frac{\partial \varphi_1}{\partial x_1} & \frac{\partial \varphi_1}{\partial x_2} \\ \frac{\partial \varphi_2}{\partial x_1} & \frac{\partial \varphi_2}{\partial x_2} \end{vmatrix} = \frac{|\mathbf{H}|}{(h_{31}x_1 + h_{32}x_2 + 1)^3}$$

Normalization of coordinates

I. translate the origin into the center of mass followed by

II. an appropriate scaling (s_1, s_2) (resp. (t_1, t_2))

AND normalize the range of nonlinear functions!!

Each equation is written in its original form

$$t_1 t_2 \sum_{m=1}^{M} \omega_i(\mathbf{Y}^m) = s_1 s_2 \sum_{n=1}^{N} \omega_i\left(\varphi(\mathbf{X}^n)\right) |J_\varphi(\mathbf{X}^n)|$$

as well as in three alternative forms

$$s_1 s_2 \sum_{n=1}^{N} \omega_i(\mathbf{X}^n) = t_1 t_2 \sum_{m=1}^{M} \omega_i\left(\varphi^{-1}(\mathbf{Y}^m)\right) |J_{\varphi^{-1}}(\mathbf{Y}^m)|$$

$$s_1 s_2 \sum_{n=1}^{N} \omega_i(\mathbf{X}^n) |J_\varphi(\mathbf{X}^n)| = t_1 t_2 \sum_{m=1}^{M} \omega_i\left(\varphi^{-1}(\mathbf{Y}^m)\right)$$

$$s_1 s_2 \sum_{n=1}^{N} \omega_i\left(\varphi(\mathbf{X}^n)\right) = t_1 t_2 \sum_{m=1}^{M} \omega_i(\mathbf{Y}^m) |J_{\varphi^{-1}}(\mathbf{Y}^m)|$$

Solving the system

- The system is solved efficiently by Levenberg-Marquardt algorithm.
- In our experiments, we have used a general initialization taking into account overall scaling.
- This proved to be efficient as long as rotation was within [-π/2, π/2].

$$\begin{pmatrix} \sqrt{\frac{t_1 t_2 M}{s_1 s_2 N}} & 0 & 0 \\ 0 & \sqrt{\frac{t_1 t_2 M}{s_1 s_2 N}} & 0 \\ 0 & 0 & 1 \end{pmatrix}$$

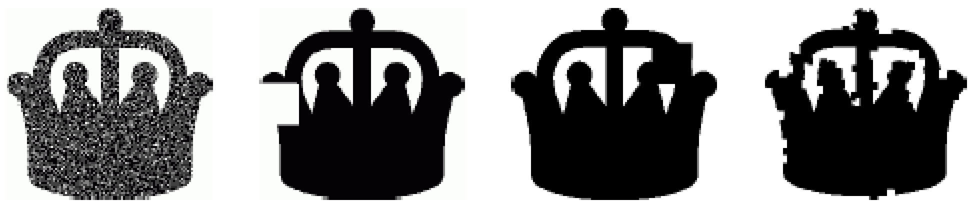

(a) missing pixels (b) occlusion (c) disocclusion (d) boundary error

Fig. 5. Sample observations with various degradations.

(a) missing pixels		5%	10%	15%	20%
Shape Context [3]	m	21.85	24.91	26.38	27.2
	σ	5.97	6.14	6.37	6.56
Proposed method	m	2.98	5.69	8.51	11.57
	σ	4.13	5.23	6.09	6.74
(b) size of occlusion		1%	2.5%	5%	10%
Shape Context [3]	m	3.03	3.55	4.55	6.79
	σ	4.79	4.79	5.09	7.03
Proposed method	m	1.41	3.40	6.19	11.27
	σ	3.49	4.18	5.09	6.6
(c) size of disocclusion		1%	2.5%	5%	10%
Shape Context [3]	m	3.63	4.52	6.25	9.28
	σ	5.19	5.61	6.84	7.78
Proposed method	m	1.93	4.54	8.28	13.62
	σ	4.31	5.13	6.16	7.09
(d) size of boundary error		1%	5%	10%	20%
Shape Context [3]	m	2.86	3.78	4.68	6.92
	σ	4.72	4.83	5.04	5.92
Proposed method	m	0.54	1.67	2.67	4.03
	σ	3.28	3.5	3.9	4.47

Traffic sign matching

- Strong deformations
- Segmentation errors
- Variations in the style of the objects (e.g. the STOP sign uses different fonts).

Thin plate spline model

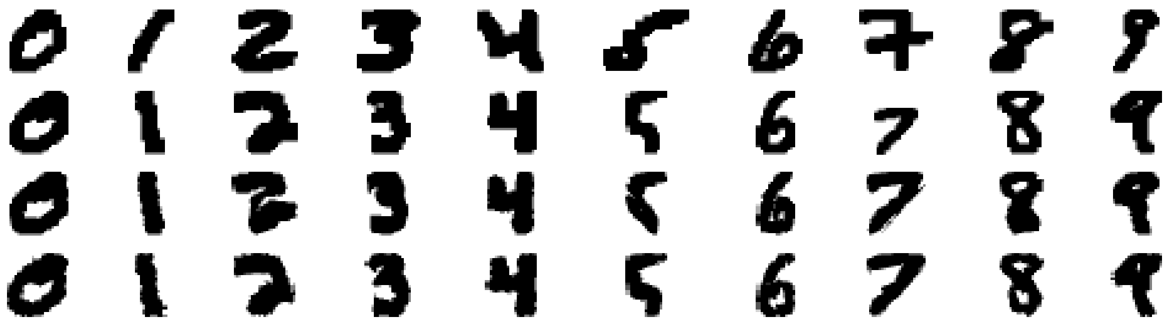

Fig. 9. Sample images from the MNIST dataset and registration results using a thin plate spline model. First and second rows show the images used as *templates* and *observations* while the 3^{rd} and 4^{th} rows show the registration results obtained by Shape Context [3] and the proposed method, respectively.

	Runtime (sec.)			δ (%)		
	m	μ	σ	m	μ	σ
Shape Context [3]	35.02	34.43	7.58	7.86	9.40	4.71
Proposed method	10.00	9.81	1.47	7.66	8.93	4.22

Aligning multimodal prostate images

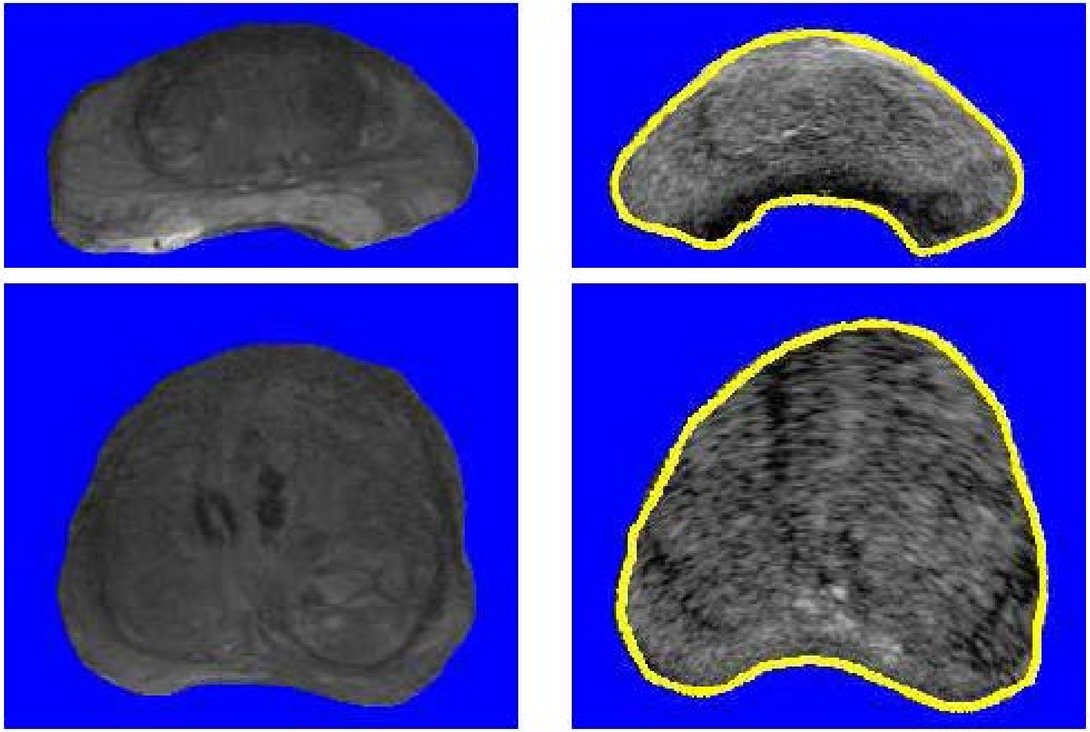

Fig. 10. Alignment of MRI (left) and US (right) prostate images using a TPS deformation model. The contours of the registered MRI images are overlaid on the US images. δ errors are 2.12% (first row) and 1.88% (second row).

Industrial inspection

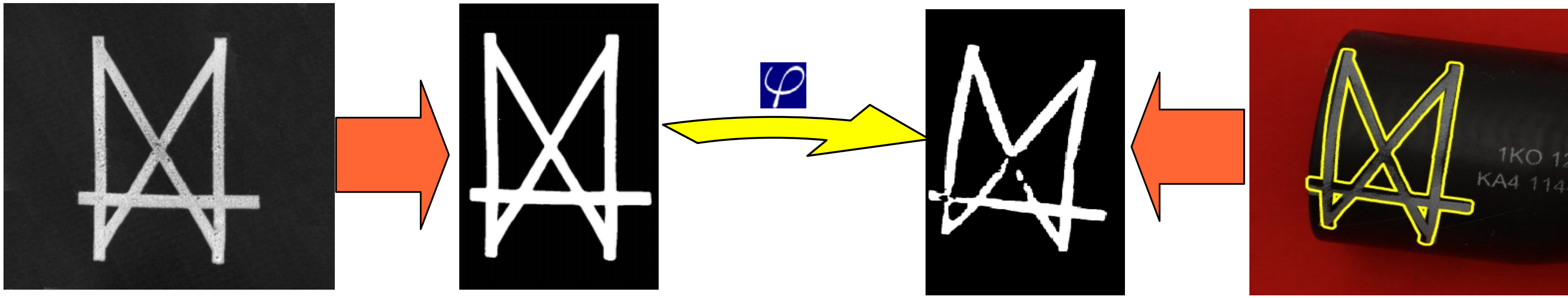

- An important step in hose manufacturing is to print various signs on the hose surface.
- The quality control in an automated inspection system can be implemented by comparing images of the printed sign to its template.
- This requires the alignment of the template and observation shapes.
- The main challenges are segmentation errors and complex distortions.

The physical model

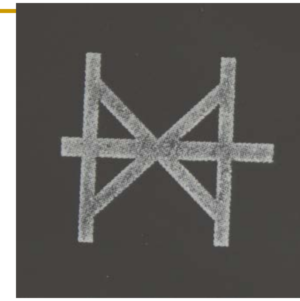

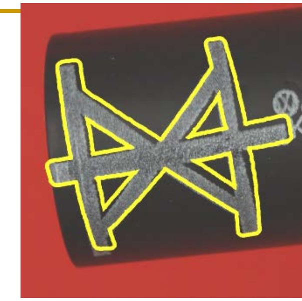

- The physical model of the contact printing procedure is as follows:
  - the stamp (basically a planar template of the sign) is positioned on the hose surface;
  - then it is pressed onto the surface.
- This procedure can be described by a sequance of transformations:
  1. $\mathbf{S} : \mathbb{R}^2 \rightarrow \mathbb{R}^2$ is a 2D rotation and scaling of the template (3 parameters)
  2. $\gamma : \mathbb{R}^2 \rightarrow \mathbb{R}^3$ maps the template's plane to a cylindric surface with radius r (1 parameter):

$$\gamma(\mathbf{x}) = \left[r \sin \frac{x_1}{r}, x_2, -r \cos \frac{x_1}{r} \right]^T$$

  3. Then a picture is taken with a camera, which is described by a classical camera matrix $\mathbf{P} : \mathbb{R}^3 \rightarrow \mathbb{R}^2$ (6 extrinsic parameters and the focal length).
- The compound transformation $\mathbf{P} \circ \gamma \circ \mathbf{S}$ acting between a planar *template* and its distorted *observation* has 11 parameters.

Industrial inspection

- Checking mounting signs on hoses used in automotive industry

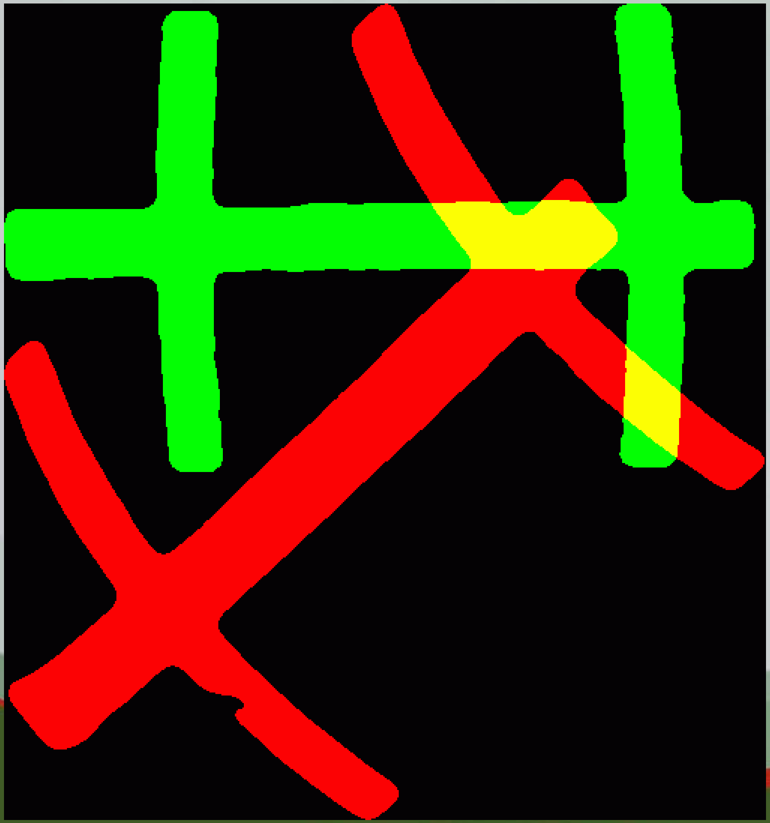

Summary

- Our method works without any
  - landmark, feature detection
  - optimization step
- The algorithm
  - works quite fast
  - is easy to implement
- Experimental results show
  - the accuracy of our method
  - the robustness of the method in the case of segmentation and modelling errors
- Current work: 3D elastic alignment without correspondences

3D polynomial deformations: preliminary results

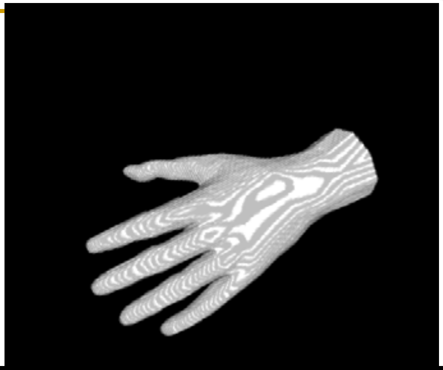

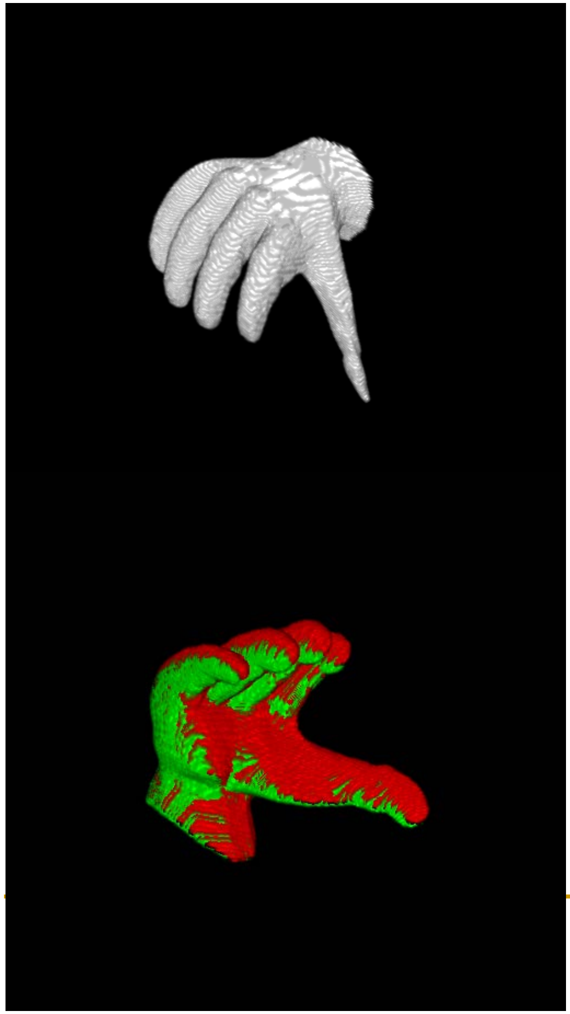

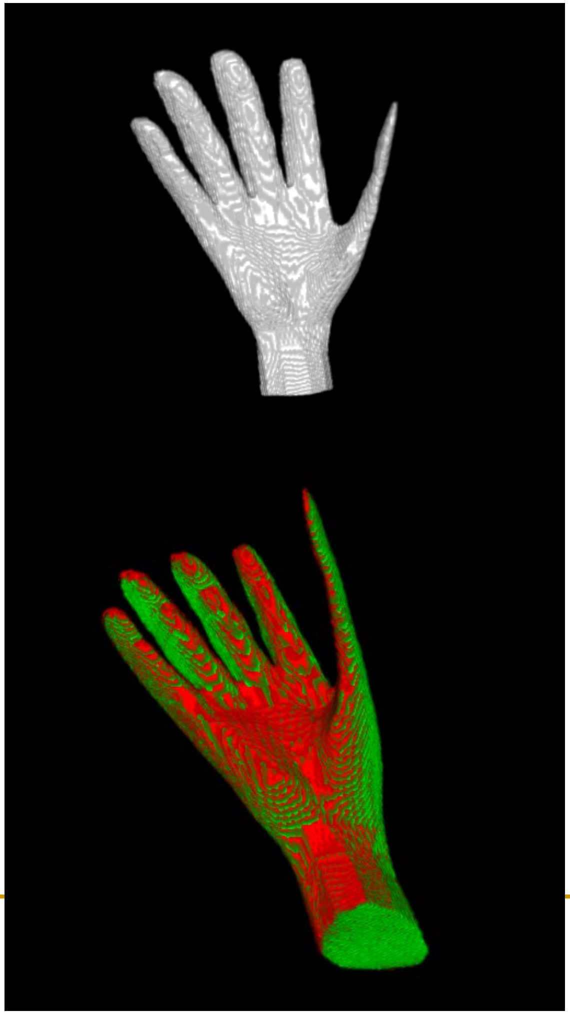

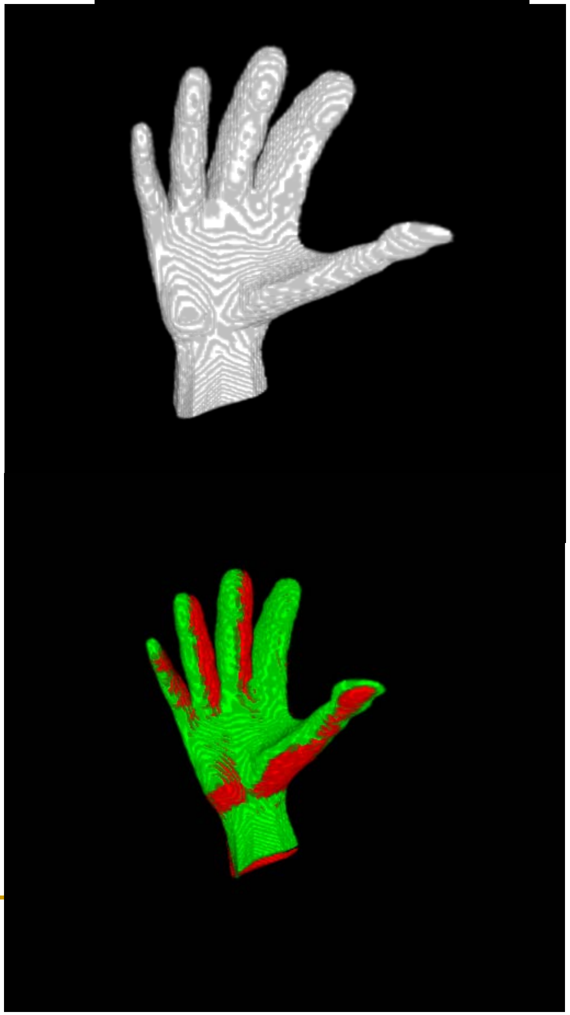

3D polynomial deformations: preliminary results

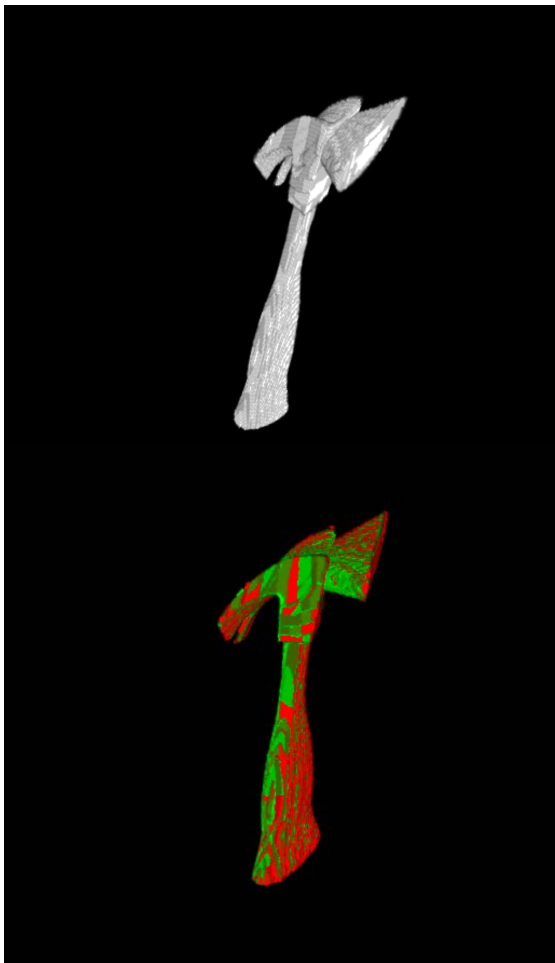

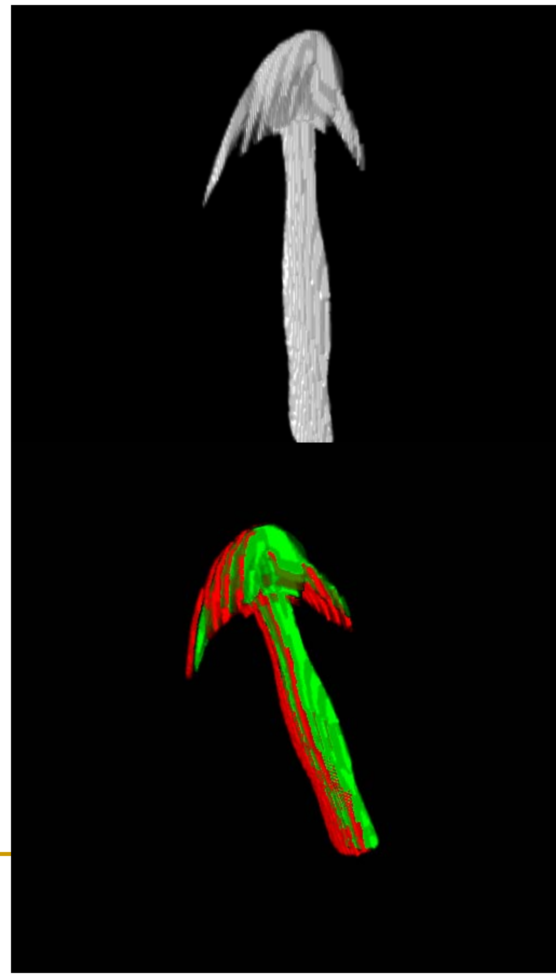

Acknowledgment

- **Csaba Domokos (PhD student), University of Szeged, Hungary**
- **Jozsef Nemeth (MSc student), University of Szeged, Hungary**
- **Attila Tanács, University of Szeged, Hungary**
- **Natasa Sladoje, University of Novi Sad, Serbia**
- **Joakim Lindblad, SUAS, Uppsala, Sweden**
- **Jhimli Mitra, Le2i-UMR CNRS 5158, Universite de Bourgogne, France**
- **Fabrice Meriaudeau, Le2i-UMR CNRS 5158, Universite de Bourgogne, France**

- **Grants:**
  - **PhD Fellowship of the Doctoral School in Informatics of the University of Szeged**
  - **Hungarian Innovation Office & Hungarian Scientific Research Fund (CNK80370)**
  - **Hungarian Scientific Research Fund (K75637)**
  - **TAMOP-4.2.2/08/1/2008-0008**
  - **TAMOP-4.2.1/B-09/1/KONV-2010-0005.**
  - ***ContiTech Fluid Automotive Hungaria Ltd.***

Publication

<u>**2D Nonlinear:**</u>

1. Csaba Domokos, Jozsef Nemeth and Zoltan Kato. **Nonlinear Shape Registration without Correspondences**. *IEEE Trans. on Pattern Analysis and Machine Intelligence*, in press, 2011.
2. Jozsef Nemeth, Csaba Domokos, and Zoltan Kato. **Nonlinear Registration of Binary Shapes**. In *Proc. **ICIP***, Cairo, Egypt, pp 1001--1004, Nov 2009. IEEE.
3. Jozsef Nemeth, Csaba Domokos, and Zoltan Kato. **Recovering Planar Homographies between 2D Shapes**. In *Proc **ICCV***, Kyoto, Japan, pp 2170--2176, Sep 2009. IEEE.

<u>**2D Affine:**</u>

1. Csaba Domokos and Zoltan Kato. **Parametric Estimation of Affine Deformations of Planar Shapes**. *Pattern Recognition*, 43(3):569--578, March 2010.
2. Csaba Domokos and Zoltan Kato. **Affine puzzle: Realigning deformed object fragments without correspondences**. In *Proc. **ECCV***, Crete, Greece, pp 777--790, Sep 2010. Springer

<u>**3D Affine:**</u>

1. Attila Tanács, Natasa Sladoje, Joakim Lindblad, and Zoltan Kato. **Estimation of Linear Deformations of 2D and 3D Fuzzy Objects**. *Pattern Recognition*, submitted, 2012
2. Attila Tanács, Natasa Sladoje, Joakim Lindblad, and Zoltan Kato. **Estimation of linear deformations of 3D objects**. In *Proc. **ICIP***, Hong Kong, China, pp 153--156, Sep 2010. IEEE.

Software

1. **Nonlinear Shape Registration without Correspondences**.
   - JAVA code.
   - Implements planar homography, extension to other nonlinear deformations is relatively easy.

2. **Affine Registration of 3D Objects**.
   - JAVA code with multi-threading (~0.2 sec. CPU time for megavoxel volumes).

3. **Affine Registration of Planar Shapes**.
   - JAVA code with a direct solver (only runs under Windows).

Available at http://www.inf.u-szeged.hu/~kato/software/